Inorganic Chemistry

Article

pubs.acs.org/IC

$Ca_{11}E_3C_8$ (E = Sn, Pb): New Complex Carbide Zintl Phases Grown from Ca/Li Flux

Trevor V. Blankenship, Adrian Lita, and Susan E. Latturner*

Department of Chemistry and Biochemistry, Florida State University, Tallahassee, Florida 32306, United States

Supporting Information

ABSTRACT: New carbide Zintl phases $Ca_{11}E_3C_8$ (E = Sn, Pb) were grown from reactions of carbon and heavy tetrelides in Ca/Li flux. They form with a new structure type in space group $P2_1/c$ (a = 13.1877(9)Å, b = 10.6915(7)Å, c = 14.2148(9)Å, β = 105.649(1)°, and R_1 = 0.019 for the $Ca_{11}Sn_3C_8$ analog). The structure features isolated E^{4-} anions as well as acetylide (C_2^{2-}) and allenylide (C_3^{4-}) anions; the vibrational modes of the carbide anions are observed in the Raman spectrum. The charge-balanced nature of these phases is confirmed by DOS calculations which indicate that the tin analog has a small band gap (E_g < 0.1 eV) and the lead analog has a pseudogap at the Fermi level. Reactions of these compounds with water produce acetylene and allene.

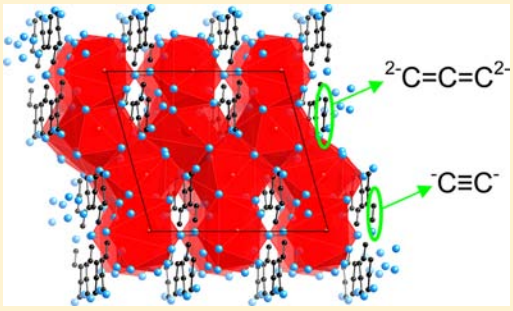

INTRODUCTION

Metal carbides, comprised of metal or metalloid elements in combination with carbon, possess very useful properties, including extreme hardness (WC, B_4C, Fe_3C), superconductivity ($LaNi_2B_2C$, Y_2C_3), and chemical inertness and high melting point (SiC).[1,2] These compounds can be grouped into several classes, depending on the nature of the metallic element in the compound. Strongly electropositive metals form salt-like carbides, ionic compounds containing discrete carbide anions such as C_2^{2-} in calcium acetylide and C_3^{4-} in Mg_2C_3. Transition metal or rare earth metal carbides (TiC, LaC_2) are usually metallic and do not follow charge-balancing rules. Carbides of semimetals such as silicon or boron are essentially covalent; the resulting network of strong localized bonds yields refractory compounds such as SiC.[1]

Due to the refractory nature of elemental carbon (often used as a crucible material for this reason), reactions to form metal carbides usually involve high temperature methods such as arc melting. However, metal flux reactions have proven to be an excellent alternative for the synthesis of new carbide phases. Reactions of carbon with other metals in eutectic melts of La/Ni (88 wt % La, mp 532 °C) have produced complex metallic carbides such as $La_{21}Fe_8Sn_7C_{12}$ and $La_{11}(MnC_6)_3$.[3,4] If a flux comprised of more electropositive metals is used, salt-like carbides are formed. Calcium metal has not been heavily explored as a solvent for metal flux reactions due to its high melting point (842 °C) and its volatility above this temperature. However, the addition of lithium to calcium results in mixtures with a dramatically lowered melting point which can be used as fluxes. The Ca/Li phase diagram features one binary intermetallic phase ($CaLi_2$); any Ca/Li mixtures with 50% Li or higher melt below 300 °C.[5] Ca/Li melts have been used as intercalation media for graphite, forming superconducting CaC_6 when graphite is soaked in Ca/Li at low temperatures (below 400 °C).[6] Our explorations of higher temperature reactions in Ca/Li mixtures have indicated that these fluxes are excellent solvents for carbon, breaking carbon sources into small reduced anions. Reactions of carbon and CaH_2 in Ca/Li flux recently yielded a complex carbide hydride phase, $LiCa_2C_3H$, containing the relatively rare C_3^{4-} anion.[7]

We have continued our explorations of carbon reactions in Ca/Li by adding heavy tetrelide reactants (tin or lead) to the flux; these reactions have produced new Zintl phase carbides $Ca_{11}E_3C_8$ (E = Sn, Pb). These compounds contain three different anionic species: monatomic E^{4-} ions and carbide anions C_2^{2-} and C_3^{4-}. The presence of two different carbide anions is highly unusual among the known metal carbides, with most examples being combinations of monatomic C^{4-} and another carbide anion (for instance, $Ca_4Ni_3C_5$ contains C^{4-} and C_2^{2-} anions; Lu_4C_7 and $Sc_5Re_2C_7$ contain C^{4-} and C_3^{4-} anions).[8,9] Besides Sc_3C_4 and its analogs (which contain C^{4-}, C_2^{2-}, and C_3^{4-}),[10] the title compounds $Ca_{11}E_3C_8$ are the only known phases to feature both acetylide (C_2^{2-}) and allenylide (C_3^{4-}) anions.

EXPERIMENTAL SECTION

Synthesis. Calcium slugs (99.5%, Alfa Aesar) were purified by heating in a steel tube under a 10^{-5} Torr vacuum at 600 °C for 3 h. Heating was continued under 10^{-3} Torr for 12 h. This process decomposes any calcium hydride and calcium oxide present and removes the resulting gaseous hydrogen and water. Chunks of Li (99.8% Strem), acetylene carbon black powder (99.5% Alfa Aesar), and either Sn (99.9% Alfa Aesar) or Pb (99.7% Fisher) granules were used as received. Reactants and flux metals were added to stainless steel crucibles (7.0 cm length/0.7 cm diameter) in a 7:7:0.7:1.9 mmol Ca/Li/E/C ratio in an argon-filled glovebox. The crucibles were sealed

Received: September 25, 2012
Published: November 21, 2012

   dx.doi.org/10.1021/ic3020833 | Inorg. Chem. 2012, 51, 13345−13350

by arc-welding under argon and were placed in silica tubes which were flame-sealed under a vacuum. The ampules were heated from room temperature to 1050 °C in 3 h and held there for 4 h. The reactions were cooled stepwise to 800 °C over 48 h, 600 °C over 144 h, and 500 °C over 72 h. The reactions were held at 500 °C and then were removed from the furnace, inverted, and centrifuged for 2 min to separate the crystalline products from the Ca/Li melt. The solid product adheres to the side of the crucible. The steel crucibles were cut open in an argon-filled glovebox. These compounds can also be synthesized in niobium crucibles to avoid the possibility of incorporation of traces of paramagnetic impurities from steel crucibles.

Elemental Analysis. Elemental analyses were performed using a JEOL 5900 scanning electron microscope with energy dispersive spectroscopy (SEM-EDS) capabilities. Samples were affixed to an aluminum SEM stub using carbon tape and analyzed using a 30 kV accelerating voltage. The atomic ratios of the tetrelide and Ca were determined with this method, but C was too light to be detected. The Ca/tetrelide ratio determined from EDS was within 5% of 70%/30%. No incorporation of elements from the steel crucible was observed in any of the samples.

Structural Characterization. Sample crystals were brought out of the glovebox under Paratone oil and were mounted in a cryoloop. Single-crystal X-ray diffraction data were collected at 170 K in a stream of nitrogen using a Bruker APEX 2 CCD diffractometer with a Mo Kα radiation source. The data were integrated with the Bruker SAINT software and corrected for absorption effects using the multiscan method (SADABS).[11] Refinement of the structure was performed using the SHELXTL package.[12] The structure was solved in monoclinic space group $P2_1/c$ (No. 14); data collection and refinement parameters are shown in Table 1. Powder X-ray diffraction studies were carried out on reaction products to identify byproducts using a Rigaku Ultima III X-ray powder diffractometer. In a glovebox, samples of solid products from each reaction were ground with a small amount of Si as an internal standard and placed in an airtight sample holder to prevent oxidation. The MDI JADE software suite was used for analysis of the powder patterns.

Table 1. Crystallographic Data and Collection Parameters for $Ca_{11}E_3C_8$ Phases

	$Ca_{11}Sn_3C_8$	$Ca_{11}Pb_3C_8$
fw (g/mol)	893.03	1158.53
cryst syst	monoclinic	monoclinic
space group	$P2_1/c$ (No.14)	$P2_1/c$ (No. 14)
a (Å)	13.1877(9)	13.2117(8)
b (Å)	10.6915(7)	10.7029(7)
c (Å)	14.2148(9)	14.2493(9)
β (°)	105.649(1)	105.650(1)
Z	4	4
volume (Å^3)	1929.9(2)	1940.2(2)
density (g/cm^3, calcd)	3.07	3.97
index ranges	$-16 < h < 16$	$-17 < h < 17$
	$-13 < k < 13$	$-14 < k < 14$
	$-18 < l < 18$	$-18 < l < 17$
reflns collected	21072	21364
unique data/params	4463/200	4536/200
μ (mm^{-1})	6.8	28.9
R_1/wR_2[a]	0.0190/0.0425	0.0259/0.0558
R_1/wR_2 (all data)	0.0202/0.0429	0.0313/0.0576
residual peak/hole (e$^-$ A^{-3})	0.78/−0.64	2.52/−1.13

[a] $R_1 = \sum||F_o| - |F_c||/\sum|F_o|$. $wR_2 = [\sum w(F_o^2 - F_c^2)^2/\sum w(F_o^2)^2]^{1/2}$.

Raman Spectroscopy. A crystal of $Ca_{11}Sn_3C_8$ was sandwiched between quartz slides which were sealed together with TorrSeal epoxy under argon. The Raman measurements were carried out using a commercial JY Horiba LabRam HR800 system excited by a HeNe laser emitting at 633 nm. The power at the sample was 28 mW. The spectrograph uses a holographic notch filter to couple the laser beam into the microscope (Olympus BX30) by total reflection. The beam is focused on the sample through a 50× IR (Leica N.A. 0.80) microscope objective. Scattered radiation is collected by the objective, and the laser radiation is filtered out by the notch filter with Raman scattering coupled into the spectrograph CCD through a confocal hole. Spectra were collected under ambient conditions over the spectral range of 50 to 3500 cm^{-1}. Attempts to collect a spectrum for the Pb analog were not successful, possibly due to its more metallic nature.

Electronic Structure Calculations. Density of states calculations were carried out using the Stuttgart TB-LMTO-ASA software package.[13] The structural models for the $Ca_{11}E_3C_8$ phases were based on the unit cell dimensions and atomic coordinates derived from single crystal diffraction data. Empty spheres were added by the program where appropriate to fill the unit cell volume. An 8 × 8 × 8 κ-point mesh was used and integrated using the tetrahedron method. The basis sets consisted of 5s/5p/5d/4f for Sn, 4s/4p/3d for Ca, and 2s/2p/3d for C. The Sn 5d/4f, Ca 4p/3d, and C 3d orbitals were downfolded.

Reactivity Studies. $Ca_{11}E_3C_8$ samples were reacted with protolytic compounds (water or NH_4Cl) to explore their interaction with the carbide anions in the structure. The reaction with water is instant and vigorous at room temperature, forming gaseous products upon the addition of 5 μL of water to 20 mg of sample in a 100 mL Schlenk flask sealed with a rubber septum under argon. Aliquots of the product gases were taken by syringe and analyzed by injecting them into a HP 6890 series GC system coupled to a HP 5973 mass selective detector. For the reaction between $Ca_{11}E_3C_8$ and NH_4Cl, 50 mg of the carbide was ground together with 50 mg of NH_4Cl in a glovebox and added to a 100 mL Schlenk flask sealed with a rubber septum. The flask was evacuated and then backfilled with nitrogen, then heated under flowing nitrogen to 200 °C using a heating mantle to induce thermal decomposition of the ammonium chloride to NH_3 and HCl. The gaseous products of the reaction of the HCl and the carbide were sampled as described for the reaction with water; both reactions gave identical products.

RESULTS AND DISCUSSION

Synthesis and Reactivity. $Ca_{11}E_3C_8$ phases form as nonfaceted elongated black chunks of about 1−2 mm in size, although some rod-like crystals are also observed (see Table 1 for crystallographic data). These phases were initially found as minor products from reactions of Ca/Li/E/C at a 10:10:1:1 mmol ratio, along with unreacted Sn or Pb and $CaSn_3$ or $CaPb_3$. The optimized synthesis ratio of carbon to heavy tetrelide is stoichiometric (7:7:0.7:1.9 mmol Ca/Li/E/C ratio), and based on these elements the yield is about 70%. The use of purified calcium metal is necessary to avoid the incorporation of adventitious hydride. If commercial (hydride-contaminated) calcium metal is used in the reaction, $LiCa_2C_3H$ is observed as a byproduct.

The $Ca_{11}E_3C_8$ phases are extremely reactive. They are air-sensitive and must be handled under an inert atmosphere. Exposure to water results in a rapid reaction to form acetylene and allene. Similar behavior is reported for other carbide phases containing C_4^{3-} units; for instance, Ln_4C_7 and $LiCa_2C_3H$ both produce C_3H_4 upon reacting with water, and hydrolysis of Sc_3C_4 yields a mixture of C_1, C_2, and C_3 hydrocarbons in accordance with the mixture of carbide anions in its structure.[7,9a,10] The mass spectra of hydrolysis products of both $Ca_{11}E_3C_8$ analogues show evidence of acetylene and propadiene (see Figure S1, Supporting Information), referenced to the corresponding spectra in the NIST database.[14] Neither stannane nor plumbane was observed. Additional peaks at 42 and 43 m/z may indicate a small amount of propene formation.

dx.doi.org/10.1021/ic3020833 | Inorg. Chem. 2012, 51, 13345−13350

Structure. $Ca_{11}E_3C_8$ (E = Sn, Pb) are, to the best of our knowledge, the only known ternary phases comprised of these elements. It is notable that no binary tin or lead carbides are known. Ternary carbides containing these elements are also rare, with M_2SnC (M = Ti, Zr, Hf, V) and the perovskite carbides R_3SnC (R = rare earth) the only reported examples; in these structures, the tin and carbon are separated by the electropositive metal.[15,16] Similarly, the new $Ca_{11}E_3C_8$ phases reported here do not feature any E−C interactions; the heavy tetrelide and carbide anions are separated from each other and coordinated only to calcium cations. This is also what is seen in $Ba_3Ge_4C_2$, the only other reported ternary carbide containing an alkaline earth metal and a heavier tetrelide element; its structure features C_2^{2-} anions and Ge_4^{4-} tetrahedral units, each surrounded by barium cations.[17]

The $Ca_{11}E_3C_8$ structure is shown in Figure 1; it forms in monoclinic space group $P2_1/c$ and features E^{4-} anions, Ca^{2+} cations, and two different types of carbide anions. The carbide anions are present as triple-bonded units of C_2^{2-} and double-bonded units of C_3^{4-}, which are deprotonated forms of acetylene and allene (propadiene), respectively. The resulting stoichiometry is charge-balanced $((Ca^{2+})_{11}(E^{4-})_3(C_2^{2-})(C_3^{4-})_2)$, with the metalloids all achieving an octet electron configuration, so these compounds can be viewed as carbide Zintl phases. While there are many known inorganic phases which incorporate organic carbon anion units, such as the metal acetylide salts with C_2^{2-} units (CaC_2, Na_2C_2, LaC_2, etc.) and Mg_2C_3 with C_3^{4-} units,[1,18] the only other reported phase that contains both C_2 and C_3 units is Sc_3C_4.[10] As shown in Figure 1b, the carbide anions in $Ca_{11}E_3C_8$ are grouped together in the same plane of near-monatomic thickness and are each surrounded by a cage of Ca cations.

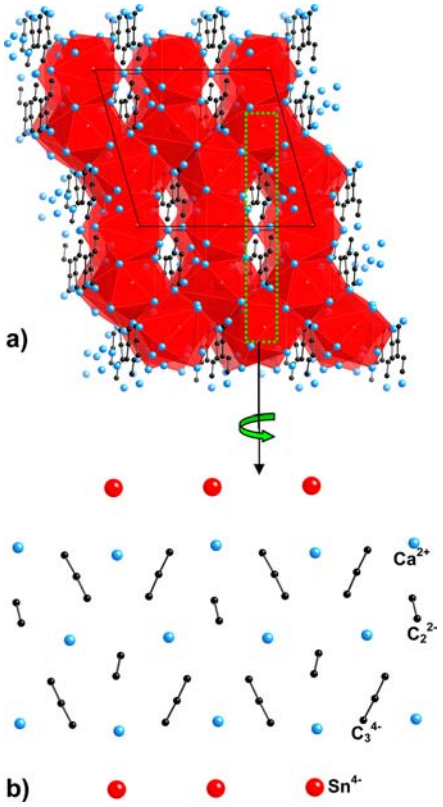

Figure 1. The structure of $Ca_{11}E_3C_8$. Carbon is represented by black spheres, E = Sn or Pb by large red spheres in coordination polyhedra, and calcium cations by blue spheres. (a) Overall monoclinic structure, viewed down the *b* axis. (b) Layer of carbide anions, viewed down the *c* axis.

The bond lengths within both of the crystallographically unique C_3^{4-} allenylide units in the $Ca_{11}E_3C_8$ structures are in the range 1.310−1.349 Å (see Figure 2 and Table 2). These values are similar to bond lengths reported for allene (1.31 Å) and other allenylide phases,[1,9,10,18] indicating that the interactions between the carbons in these anions are double bonds. It is notable that the bond lengths from the central carbon to the two terminal carbon atoms are slightly different. Most other reported ionic allenylides have identical bond

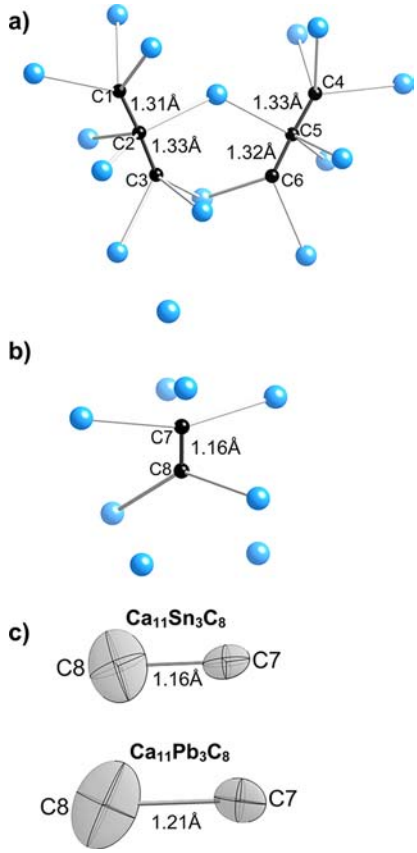

Figure 2. Carbide anions in $Ca_{11}Sn_3C_8$, with carbon−carbon bond lengths indicated. Calcium cations depicted as blue spheres. (a) Allenylide (C_3^{4-}) anions. (b) Acetylide (C_2^{2-}) anion. (c) Acetylide anions for the tin and lead analogs, displaying displacement ellipsoids.

Table 2. Bond Lengths of Interest in $Ca_{11}E_3C_8$ Phases, in Angstrom Units

bond	$Ca_{11}Sn_3C_8$	$Ca_{11}Pb_3C_8$
E1−Ca	3.1594(5)−3.7644(6)	3.179(1)−3.777(1)
E2−Ca	3.1388(5)−3.7612(6)	3.153(1)−3.763(1)
E3−Ca	3.1835(5)−3.8122(6)	3.193(1)−3.828(1)
Ca−C	2.437(2)−2.896(2)	2.446(6) −2.899(6)
C1−C2	1.313(3)	1.314(8)
C2−C3	1.329(3)	1.349(8)
C4−C5	1.328(3)	1.327(8)
C5−C6	1.320(3)	1.310(8)
C7−C8	1.155(5)	1.21(1)

dx.doi.org/10.1021/ic3020833 | *Inorg. Chem.* 2012, 51, 13345−13350

lengths, with the central carbon atom often lying on an inversion center or mirror plane. All C_3^{4-} anions in the $Ca_{11}E_3C_8$ phases are slightly bent with angles ranging from 174.4 to 176.1°. The allenylide ions are in a cage of nine Ca^{2+} cations; terminal carbon atoms are bonded to three Ca^{2+} ions in a pyramidal geometry, and the central carbon atom is bonded to three Ca^{2+} ions in a trigonal planar geometry. These cations are in a staggered arrangement with the ones on the end. The Ca−C bonds range from 2.437(2) to 2.657(2)Å for $Ca_{11}Sn_3C_8$ and 2.446(6) to 2.663(6)Å for $Ca_{11}Pb_3C_8$. A similar arrangement of Ca^{2+} cations around a C_3^{4-} unit is found in $Ca_3C_3Cl_2$, which has three Ca^{2+} ions coordinating the end carbon atoms but only two Ca^{2+} ions coordinated to the central carbon atom.[19,20]

The bond distance for the C_2^{2-} unit in $Ca_{11}Sn_3C_8$ (1.155(4) Å) is smaller than the usual bond length of 1.19 Å seen in ionic acetylides.[1] This can be explained by disorder in the atom positions of this unit, indicated by the large displacement parameters of the carbon atoms (see Figure 2c). The bond distance is calculated from the centroid of the displacement ellipsoids around the carbon atoms, but depending on the actual location of the carbon atom the effective bond length will be longer. This effect has also been reported for C_2^{2-} units in $Ca_5Cl_3(C_2)(CBC)$ and $Ca_{15}(CBN)_6(C_2)_2O$, which have disorder-averaged bond lengths of 1.08 and 1.095 Å, respectively.[21,22] The acetylide anion in the Pb analogue does not exhibit as much disorder. Accordingly, its bond distance (1.21(1) Å) is within the range expected for a triple bond.

The heavy tetrelide elements form isolated E^{4-} anions bonded solely to calcium cations in 10-coordinate arrangements. The high negative charge on these anions is evidence of the strong reducing power and large excess of the Ca/Li flux reaction medium. This is in contrast to the larger anionic clusters often found in tetrelide Zintl phases, such as Pb_4^{4-} (seen in KPb) and Sn_9^{4-} (seen in $Rb_{12}Sn_{17}$), which have a smaller negative charge per atom.[23,24] The calcium coordination of all three crystallographically unique tetrelide sites can be described roughly as bicapped square antiprismatic; an example is shown in Figure 3. The Sn−Ca bond distances range from

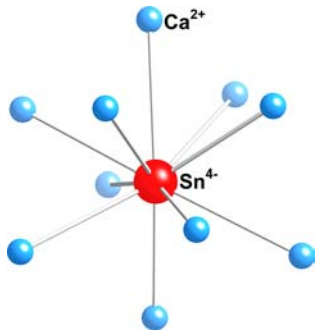

Figure 3. Bicapped square antiprism coordination of an E^{4-} anion (red sphere) by calcium (blue spheres) in $Ca_{11}E_3C_8$ phases.

3.1388(5) to 3.8122(6) Å, and the Pb−Ca bond distances range from 3.153(1) to 3.828(1) Å. Bond distances from literature range between 3.1 and 3.72 Å for Ca−Sn bonds and 3.1 and 3.76 for Ca−Pb bonds but are usually below 3.5 Å.[25,26]

Raman Spectrum. The Raman spectrum of $Ca_{11}Sn_3C_8$ (Figure 4) confirms the presence of double and triple bonds in the carbide anions. The acetylide anion stretch (1879 cm^{-1}) is within the 1800−1900 cm^{-1} range observed for binary alkali

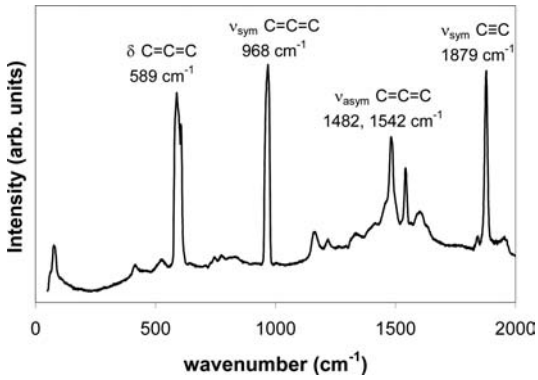

Figure 4. Raman spectrum of $Ca_{11}Sn_3C_8$.

metal acetylides, which is significantly downshifted from the range typical for neutral organic alkynes (2100−2300 cm^{-1}) due to the higher negative charge for anionic species.[1] Similarly, the C_3^{4-} allenylide stretching modes in $Ca_{11}Sn_3C_8$ (ν_{sym} 968 cm^{-1}, ν_{asym} 1482, 1542 cm^{-1}) occur at lower energy than the typical alkene range of 1600−1700 cm^{-1}. The only previous report on vibrational spectra of a phase containing the C_3^{4-} anion is for $Ca_3C_3Cl_2$, which exhibits ν_{sym} 1159 cm^{-1} and ν_{asym} 1660 cm^{-1}.[20,27] While the observed allenylide modes for $Ca_{11}Sn_3C_8$ are significantly different from those stated for $Ca_3C_3Cl_2$, the Raman spectrum in Figure 4 is very similar to those seen for $Ca_{15}(CBN)_6(C_2)_2X_2$ (X = F or H). These complex salts feature linear, double bonded CBN^{4-} anions (isoelectronic with C_3^{4-}), acetylide anions, and either fluoride or hydride anions.[27,28] The hydride analog exhibits a C_2^{2-} stretching mode at 1879 cm^{-1}, identical to that for $Ca_{11}Sn_3C_8$. The CBN^{4-} anion ν_{asym} modes (at 1482 and 1543 cm^{-1}), ν_{sym} stretch (970 cm^{-1}), and bending mode (605 cm^{-1}) all correspond very well to the Raman modes for the allenylide anion in $Ca_{11}Sn_3C_8$.[28]

The Raman spectrum in Figure 4 shows an additional peak at 80 cm^{-1}. This may be due to a rattling mode of the stannide anions. No vibrational spectra are available for Ca_2Sn, but Mg_2Sn exhibits a Raman mode at 222 cm^{-1}, and the corresponding mode for the heavier calcium analog would be expected to be shifted to lower energy.[29] This mode might be analogous to that of heavy anions in inverse clathrate cages (such as I^- anions in the cages of $I_8Sb_8Ge_{38}$), which exhibit rattling vibrations below 100 cm^{-1}.[30]

Electronic Structure. Density of states data for the $Ca_{11}E_3C_8$ phases are shown in Figure 5. DOS diagrams of both analogs feature small band gaps or pseudo band gaps at the Fermi level (E_g = 0.1 eV for the tin phase and a pseudogap for the lead analog), in agreement with their charge-balanced stoichiometries and black color. Bands associated with calcium and the heavy tetrelide anions are prevalent just below E_f. States derived from carbide anion orbitals are found at lower energies (between −2 and −4 eV below E_f for the tin analog). This is in agreement with the higher electronegativity of carbon compared to the heavier tetrelide elements; the carbide associated bands are also considerably narrower (electrons more localized) than the E^{4-} bands. The data compare well to calculations carried out on binary phases Ca_2Sn and CaC_2. Ca_2Sn features tin anions surrounded by nine calcium cations in a tricapped trigonal prism coordination. It is a very narrow band gap semiconductor (E_g = 0.1 eV), with states derived from Sn p orbitals predominant just below E_f and empty Ca bands above

dx.doi.org/10.1021/ic3020833 | Inorg. Chem. 2012, 51, 13345−13350

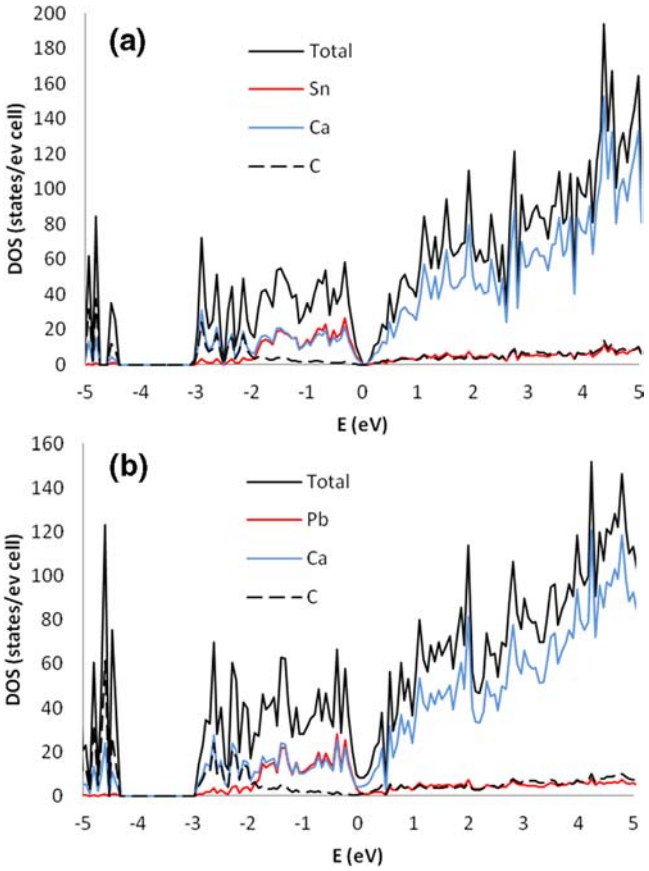

Figure 5. Density of states data for $Ca_{11}Sn_3C_8$ (a) and $Ca_{11}Pb_3C_8$ (b).

the gap, as is also seen for $Ca_{11}Sn_3C_8$.[31] CaC_2 has a tetragonal distorted NaCl structure type, with C_2^{2-} anions aligned along the *c* axis in octahedral coordination by Ca^{2+} ions. The energy difference between states derived from filled acetylide anion orbitals and empty calcium bands is considerable; this colorless compound has a bandgap over 3 eV.[32] This supports the observed relative energies of carbon- and tin-derived valence bands with respect to the calcium-based states in the conduction band of $Ca_{11}Sn_3C_8$.

CONCLUSIONS

Calcium/lithium melts have proven to be excellent reaction media for the synthesis of new complex carbide phases. Reactions at high temperatures have produced several new compounds featuring the relatively rare C_3^{4-} anion, including the $Ca_{11}E_3C_8$ title compounds and $LiCa_2C_3H$.[7] Variation of the reaction temperature and carbon source may allow for the formation of phases with larger carbide anions. $Ca_{11}E_3C_8$ phases are highly reactive toward electrophiles. The presence of two different carbide anions and their packing in the unit cell may make these compounds useful precursors for the synthesis of complex organic molecules.

ASSOCIATED CONTENT

Supporting Information

Tables of atomic positions, mass spectrum from hydrolysis of $Ca_{11}Pb_3C_8$, and crystallographic data for both phases as CIF files. This material is available free of charge via the Internet at http://pubs.acs.org

AUTHOR INFORMATION

Corresponding Author

*Phone: 850-644-4074. Fax: 850-644-8281. E-mail: latturne@chem.fsu.edu.

Notes

The authors declare no competing financial interest.

ACKNOWLEDGMENTS

This research was supported by funding from the National Science Foundation (Division of Materials Research) through grant numbers DMR-05-47791 and DMR-11-06150 and by the FSU Department of Chemistry and Biochemistry. This research made use of the scanning electron microscope facilities of the FSU Physics Department.

REFERENCES

(1) Ruschewitz, U. *Coord. Chem. Rev.* **2003**, *244*, 115−136.
(2) Simon, A. *Angew. Chem., Int. Ed.* **1997**, *36*, 1788−1806.
(3) Benbow, E. M.; Dalal, N.; Latturner, S. E. *J. Am. Chem. Soc.* **2009**, *131*, 3349−3354.
(4) Zaikina, J. V.; Zhou, H.; Latturner, S. E. *J. Solid State Chem.* **2010**, *183*, 2987−2994.
(5) Massalski, T. B.; Okamoto, H. *Binary Alloy Phase Diagrams*, 2nd ed.; ASM International: Materials Park, OH, 1990.
(6) Emery, N.; Herold, C.; Lagrange, P. *Prog. Solid State Chem.* **2008**, *36*, 213−222.
(7) Lang, D. A.; Zaikina, J. V.; Lovingood, D. D.; Gedris, T. E.; Latturner, S. E. *J. Am. Chem. Soc.* **2010**, *132*, 17532−17530.
(8) Musanke, U. E.; Jeitschko, W. *Z. Naturforsch. B* **1991**, *46*, 1177.
(9) (a) Czekalla, R.; Jeitschko, W.; Hoffmann, R. D.; Rabeneck, H. *Z. Naturforsch. B* **1996**, *51*, 646−654. (b) Pöttgen, R.; Jeitschko, W. *Z. Naturforsch. B* **1992**, *47*, 358−364.
(10) Pöttgen, R.; Jeitschko, W. *Inorg Chem.* **1991**, *30*, 427−431.
(11) *SAINT*, version 6.02a; Bruker AXS Inc.: Madison, WI, 2000.
(12) Sheldrick, G. M. *SHELXTL NT/2000*, version 6.1; Bruker AXS, Inc.: Madison, WI, 2000.
(13) (a) Jepsen, O.; Burkhardt, A.; Andersen, O. K. *The Program TB-LMTO-ASA*, version 4.7; Max-Planck-Institut für Festkörperforschung: Stuttgart, Germany, 2000. (b) Blöchl, P. E.; Jepsen, O.; Andersen, O. K. *Phys. Rev. B* **1994**, *49*, 16223−16233.
(14) Stein, S. E. Mass Spectra. In *NIST Chemistry WebBook, NIST Standard Reference Database Number 69*; Linstrom, P. J., Mallard, W. G., Eds.; National Institute of Standards and Technology: Gaithersburg, MD. http://webbook.nist.gov (accessed Nov. 2012).
(15) Jeitschko, W.; Nowotny, H. N.; Benesovsky, F. *Monatsh. Chem.* **1963**, *94*, 672−676.
(16) Haschke, H.; Nowotny, H. N.; Benesovsky, F. *Monatsh. Chem.* **1966**, *97*, 1045.
(17) Curda, J.; Carrillo-Cabrera, W.; Schmeding, A.; Peters, K.; Somer, M.; von Schnering, H. G. *Z. Anorg. Allg. Chem.* **1997**, *623*, 929−936.
(18) Fjellvaag, H.; Karen, P. *Inorg. Chem.* **1992**, *31*, 3260−3263.
(19) Hoffmann, R.; Meyer, H. J. *Z. Anorg. Allg. Chem.* **1992**, *607*, 57−71.
(20) Meyer, H. J. *Z. Anorg. Allg. Chem.* **1991**, *593*, 185−192.
(21) Reckeweg, O.; Meyer, H. J. *Angew. Chem., Int. Ed.* **1998**, *37*, 3407−3410.
(22) Wörle, M.; Muhr, H. J.; Altenschildesche, H. M. Z.; Nesper, R. *J. Alloys Compd.* **1997**, *260*, 80−87.
(23) Röhr, C. *Z. Naturforsch. B* **1995**, *50*, 802−808.
(24) Hoch, C.; Wendorff, M.; Röhr, C. *J. Alloys Compd.* **2003**, *361*, 206−221.
(25) Eckerlin, P.; Leicht, E.; Wolfel, E. Z. *Anorg. Allg. Chem.* **1961**, *307*, 145−156.
(26) Bruzzone, G.; Merlo, F. J. *J. Less-Common Met.* **1976**, *48*, 103−109.

(27) Reckeweg, O.; Schulz, A.; DiSalvo, F. J. *Z. Naturforsch.* **2010**, *65b*, 1409−1415.
(28) Reckeweg, O.; Schulz, A.; DiSalvo, F. J. *Z. Naturforsch.* **2011**, *66b*, 1092−1096.
(29) Buchenauer, C. J.; Cardona, M. *Phys. Rev. B* **1971**, *3*, 2504−2507.
(30) Shimizu, H.; Oe, R.; Ohno, S.; Kume, T.; Sasaki, S.; Kishimoto, K.; Koyanagi, T.; Ohishi, Y. *J. Appl. Phys.* **2009**, *105*, 043522.
(31) (a) Yang, Z.; Shi, D.; Wen, B.; Melnik, R.; Yao, S.; Li, T. *J. Solid State Chem.* **2010**, *183*, 136−143. (b) Migas, D. B.; Miglio, L.; Shaposhnikov, V. L.; Borisenko, V. E. *Phys. Rev. B* **2003**, *67*, 205203.
(32) Ruiz, E.; Alemany, P. *J. Phys. Chem.* **1995**, *99*, 3114−3119.